



ISSN 0975-413X
CODEN (USA): PCHHAX

Der Pharma Chemica, 2016, 8(4):226-236
(<http://derpharmachemica.com/archive.html>)

Some quinoline derivatives: Synthesis and comparative study towards corrosion of mild steel in 0.5 H₂SO₄

A. Elyoussfi¹, A. Dafali¹, H. Elmsellem¹, Y. Bouzian², R. bouhfid³, A. Zarrouk¹,
K.Cherrak¹, E. M. Essassi², A. Aouniti¹ and B. Hammouti¹

¹Laboratoire de chimie analytique appliquée, matériaux et environnement (LC2AME), Faculté des Sciences, B.P. 717, 60000 Oujda, Morocco

²Laboratoire de Chimie Organique Hétérocyclique, URAC 21, Pôle de Compétences Pharmacochimie, Université Mohammed V, Faculté des Sciences, Av. Ibn Battouta, BP 1014 Rabat, Morocco

³Moroccan Foundation for Advanced Science, Innovation and Research (MASCIR), Institut of Nanomaterials and Nanotechnology, Rabat, Morocco

ABSTRACT

Adsorption of two derivatives of quinoline on mild steel surface in 0.5 H₂SO₄ solution and its corrosion inhibition properties has been studied by a series of techniques, such as polarization, electrochemical impedance spectroscopy (EIS), weight loss and quantum chemical calculation methods. Potentiodynamic polarization measurements showed that all inhibitors are cathodic type. The degree of surface coverage was determined by using weight loss measurements and it was found that adsorption process of studied inhibitors on mild steel surface obeys Langmuir adsorption isotherm.

Keywords: quinoline derivatives; steel; Hydrochloric acid; Corrosion inhibition; Adsorption; DFT.

INTRODUCTION

An important practical application of such phenomena is corrosion inhibition. Numerous investigations have been performed on the inhibition of mild steel and steel alloy by using of organic compounds [1- 3]. Molecular structure of inhibitors has clearly been established as a major influence on corrosion inhibition. Heteroatom's as oxygen, nitrogen, phosphorus and sulfur as well as aromatic ring in their structure are the major adsorption centres.

The objective of this work is to study the influence of quinoline derivatives on the corrosion of mild steel in 0.5M H₂SO₄ at different concentrations of inhibitors by electrochemical measurements: weight loss, polarization curve and electrochemical impedance spectroscopy. Quantum chemical studies were also carried out to propose an interpretation of the data.

MATERIALS AND METHODS

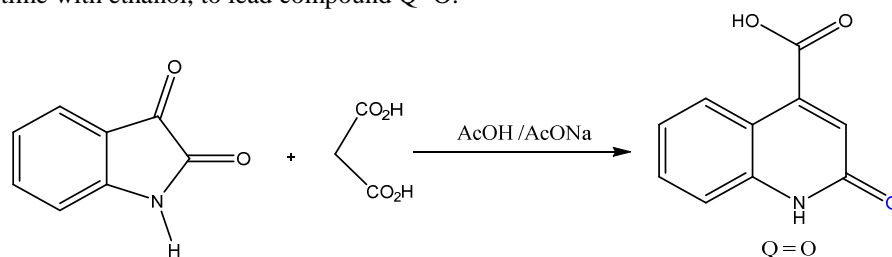
2.1. Materials

Mild steel was used for this study has the following composition: (0.37% C, 0.23%Si, 0.016 S%, 0,68 Mn%, 0.16 Cu%, 0.077Cr%, 0.011Ti%, 0,052Ni%, 0.009 Co%) The specimen was used for electrochemical measurements. The exposed surface area was 1cm².

2.2. Synthesis of inhibitors

2.2.1 Synthesis of 2-oxo-1,2-dihydroquinoline-4-carboxylic acid (Q = O)

To a solution of isatin (10 mmole) and malonic acid (10 mmole) in acetic acid 30 ml, was added sodium acetate (1 mmole). The mixture was refluxed for 24 hours. After cooling ice-water (100ml) was added. The obtained precipitate washed several time with ethanol, to lead compound Q=O.

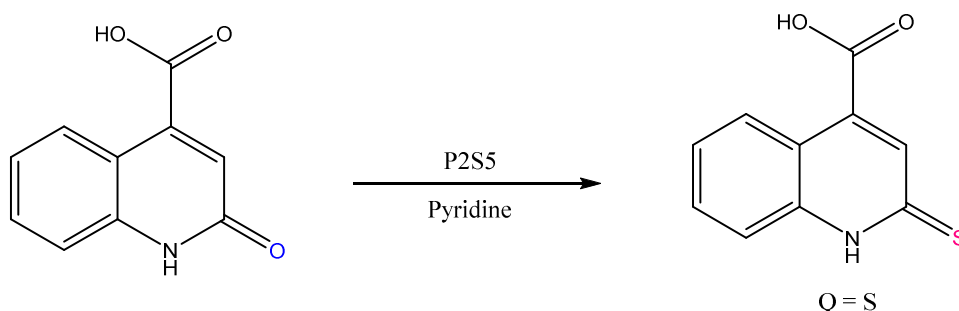


Scheme 1: Synthesis of 2-oxo-1,2-dihydroquinoline-4-carboxylic acid (Q = O)

Rdt = 87 %. F > 250 °C (EtOH). Spectre de RMN 1H (DMSOd6) : 7.14(s, 1H, CH); 7.68-8.63(m, 4H, CHAr). Spectre de RMN 13C (DMSOd6) : 120.6 (=CH); 117.1, 117.6, 126.7, 133.7 (CHAr); 118.3, 137.0, 142.7 (Cq); 163.5 (C=O); 169.5 (CO2H). Spectre IR (cm-1) 3210 vN-H ; 2900-3100 vO-H ; 1705 vC=O. Spectre de masse (IE) M (m/z) = 189.

2.2.2. Synthesis of 2-thioxo-1,2-dihydroquinoline-4-carboxylic acid (Q = S)

To a well-stirred solution of (5 g, 33.1mmol) 2-oxo-1,2-dihydroquinoline-4-carboxylic acid in 50 mL of dry pyridine was added (14.7 g, 33.1mmol) phosphorus pentasulfide. The reaction mixture is heated to reflux for 4 hours, the solid obtained is washed several times with hot water, dried and then purified in absolute ethanol. Recrystallization is carried out in the petroleum ether. The product obtained was characterized by ¹H NMR, ¹³C NMR.



Scheme 2: Synthesis of 2-thioxo-1,2-dihydroquinoline-4-carboxylic acid (Q = S)

Rdt = 90 %. ¹H NMR (DMSOd6): 7.41(s, 1H, CH); 7.28-8.5(m, 4H, CH_{Ar}). ¹³C NMR(DMSOd6): 121.6 (=CH); 117.2, 126.1, 127.0, 128.3 (CH_{Ar}); 122.7, 134.5, 140.2 (Cq); 191.4 (C=O); 166.1 (CO₂H). ESI-MS MH m/z = 206.23.

2.3. Solutions

The aggressive solution of 1.0 M H₂SO₄ was prepared by dilution of analytical grade 98% H₂SO₄ with distilled water. The concentration range of inhibitors is 10⁻⁶-10⁻³ (M).

2.4. Weight loss Method

Coupons were cut into 1.5 × 1.5 × 0.05 cm³ dimensions having composition (0.09%P, 0.01 % Al, 0.38 % Si, 0.05 % Mn, 0.21 % C, 0.05 % S and Fe balance) used for weight loss measurements. Prior to all measurements, the exposed area was mechanically abraded with 180, 400, 800, 1000, 1200 grades of emery papers. The specimens are washed thoroughly with bidistilled water degreased and dried with ethanol. Gravimetric measurements are carried out in a double walled glass cell equipped with a thermostated cooling condenser. The solution volume is 100 cm³. The immersion time for the weight loss is 6 h at (308±1) K. In order to get good reproducibility, experiments were carried out in duplicate. The average weight loss was obtained. The corrosion rate (v) is calculated using the following equation:

$$v = W / S.t \quad (1)$$

Where W is the average weight loss, S the total area, and t is immersion time. With the corrosion rate calculated, the inhibition efficiency (E_w) is determined as follows:

$$E_w \% = \frac{V_0 - V}{V_0} \times 100 \quad (2)$$

Where V_0 and V are the values of corrosion rate without and with inhibitor, respectively.

2.5. Electrochemical measurements

The electrochemical study was carried out using a potentiostat PGZ100 piloted by Voltmaster soft-ware. This potentiostat is connected to a cell with three electrode thermostats with double wall. A saturated calomel electrode (SCE) and platinum electrode were used as reference and auxiliary electrodes, respectively. Anodic and cathodic potentiodynamic polarization curves were plotted at a polarization scan rate of 0.5mV/s. Before all experiments, the potential was stabilized at free potential during 30 min. The polarisation curves are obtained from -800 mV to -200 mV at 308 K. The solution test is there after de-aerated by bubbling nitrogen. Inhibition efficiency (E_p %) is defined as:

$$E_p \% = \frac{i_{cor(0)} - i_{cor(inh)}}{i_{cor(0)}} \times 100 \quad (3)$$

Where $i_{cor(0)}$ and $i_{cor(inh)}$ represent corrosion current density values without and with inhibitor, respectively.

The electrochemical impedance spectroscopy (EIS) measurements are carried out with the electrochemical system, which included a digital potentiostat model Voltalab PGZ100 computer at E_{corr} after immersion in solution without bubbling. After the determination of steady-state current at a corrosion potential, sine wave voltage (10 mV) peak to peak, at frequencies between 100 kHz and 10 mHz are superimposed on the rest potential. Computer programs automatically controlled the measurements performed at rest potentials after 0.5 hour of exposure at 308 K. The impedance diagrams are given in the Nyquist representation.

Inhibition efficiency (E_R %) is estimated using the relation:

$$E_R \% = \frac{R_t(inh) - R_t(0)}{R_t(inh)} \times 100 \quad (4)$$

Where $R_t(0)$ and $R_t(inh)$ are the charge transfer resistance values in the absence and presence of inhibitor, respectively.

2.6. Computational Chemistry

The quantum chemical calculations, of quinoline derivatives, reported in this work are performed at the B3LYP/6-31G (d,p) level of theory using Gaussian 09 series of programs[4,5].

RESULTS AND DISCUSSION

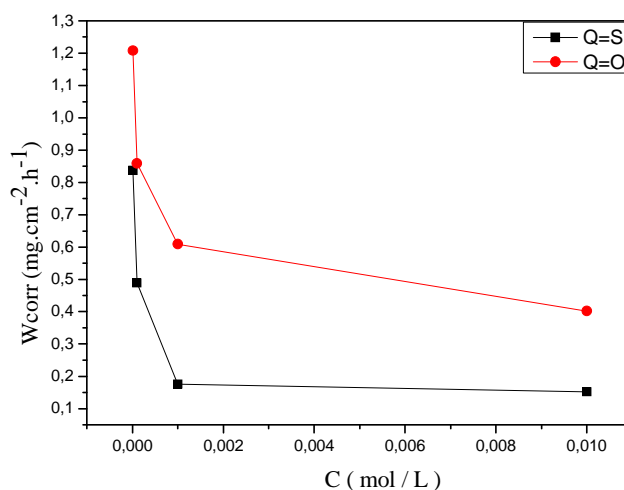
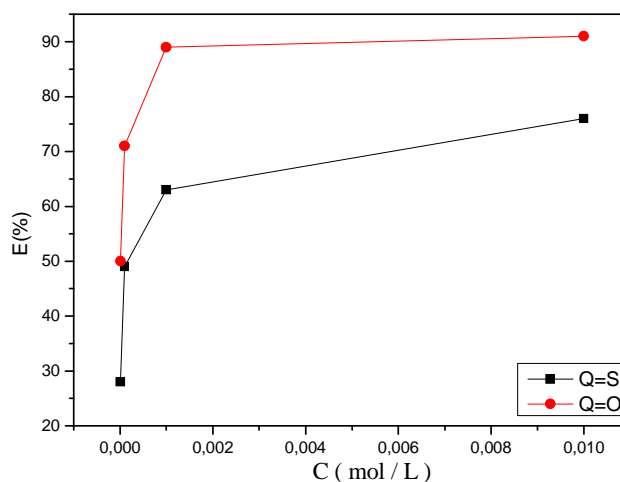
3.1. Gravimetric study

Figure 1 illustrates the corrosion rate of mild steel in 0.5 M H_2SO_4 at 308K in the presence of different concentrations of quinoline derivatives. The corrosion rate reduces after addition of the selected two quinoline derivatives, and decreases with the inhibitor concentration due to the fact that the adsorption coverage increases, which shields the mild steel surface efficiently from the medium. In the absence of inhibitor, the corrosion rate is $1.69 \text{ mg.cm}^{-2}.\text{h}^{-1}$. While in the presence of 10^{-3} M inhibitor, the corrosion rate values are reduced to 0.152 and 0.402 $\text{mg.cm}^{-2}.\text{h}^{-1}$, for Q=S and Q=O, respectively. At any given inhibitor concentration, the corrosion rate follows the order: Q=S < Q=O, which indicates that Q=S exhibits the best inhibitive performance among two quinoline compounds.

Figure 2 represents inhibition efficiency values obtained from the weight loss(E_w) in 0.5 M H_2SO_4 solutions in the presence of various concentrations of Q=S and Q=O at 308K. Clearly, E_w increases with an increase in the inhibitor concentration. It should be noted that when the concentration of inhibitor reaches about 10^{-3} M, E_w reaches certain value and change slightly with a further increase in the inhibitor concentration. At 10^{-3} M, the maximum E_w is 91% for Q=S and 76% for Q=O, which indicates all quinoline compounds act as good corrosion inhibitors for mild steel in 0.5 M H_2SO_4 . E_w values of the examined quinoline derivatives follow the order: Q=S > Q=O.

Table 1: Corrosion parameters obtained from weight loss measurements for carbon steel in 0.5 M H₂SO₄ containing various concentration of inhibitor at 308 K

Inhibiteur	Concentration (M)	W _{corr} (mg.cm ⁻² .h ⁻¹)	E _w (%)	θ
0.5 M H ₂ SO ₄	--	1.69	--	--
Q=S	10 ⁻⁶	0.837	50	0.50
	10 ⁻⁵	0.489	71	0.71
	10 ⁻⁴	0.176	89	0.89
	10 ⁻³	0.152	91	0.91
Q=O	10 ⁻⁶	1.208	28	0.28
	10 ⁻⁵	0.859	49	0.49
	10 ⁻⁴	0.609	63	0.63
	10 ⁻³	0.402	76	0.76

**Figure 1. Relationship between the corrosion rate and inhibitor concentration for steel after 6 h immersion in 0.5 M H₂SO₄ at 308 K****Figure 2. Relationship between the inhibition efficiency and inhibitors concentration for mild steel after 6 h immersion in 0.5M H₂SO₄ at 308 K**

3.2. Adsorption isotherm and standard adsorption free energy

Basic information on the adsorption of inhibitor on metal surface can be provided by adsorption isotherm. Several isotherms including Frumkin, Langmuir, Temkin, Freundlich, Bockris–Swinkels and Flory–Huggins isotherms are employed to fit the experimental data. It is found that the adsorption of studied inhibitors on steel surface obeys the Langmuir adsorption isotherm equation [6]:

$$\frac{C}{\theta} = \frac{1}{k} + C \quad (5)$$

where c is the concentration of inhibitor, K the adsorption equilibrium constant, and h is the surface coverage and expressed by the ration $E_w\%/100$.

Plots of C/θ against c yield straight lines as shown in Figure 3, and the corresponding linear regression parameters are listed in Table 2. Both linear correlation coefficient (r) and slope are close to 1, indicating the adsorption of three quinoline inhibitors on mild steel surface obeys Langmuir adsorption isotherm. Also, K follows the order: $Q=S > Q=O$. Generally, large value of K means better inhibition performance of a given inhibitor. This is in good agreement with the values of E_w obtained from Figure 3.

The adsorption equilibrium constant (K) is related to the standard adsorption free energy (ΔG°) as shown the following equation [7]:

$$K = \frac{1}{55.55} \exp\left(-\frac{\Delta G_{ads}^\circ}{RT}\right) \quad (6)$$

where R is the gas constant ($8.314 \text{ J K}^{-1} \text{ mol}^{-1}$), T the absolute temperature (K), and the value 55.5 is the concentration of water in the solution expressed in M [7]. The ΔG° values are also presented in Table 2. Furthermore, values of ΔG° up to -20 kJ mol^{-1} are consistent with the electrostatic interaction between the charged molecules and the charged metal (physisorption) while those more negative than -40 kJ mol^{-1} involve sharing or transfer of electrons from the inhibitor molecules to the metal surface to form a co-ordinate type of bond (chemisorption) [8]. In the present study, the value of ΔG° is found to be within the range from -40 kJ mol^{-1} ; probably means that the adsorption of each quinoline inhibitor on the mild steel surface contains chemical adsorption.

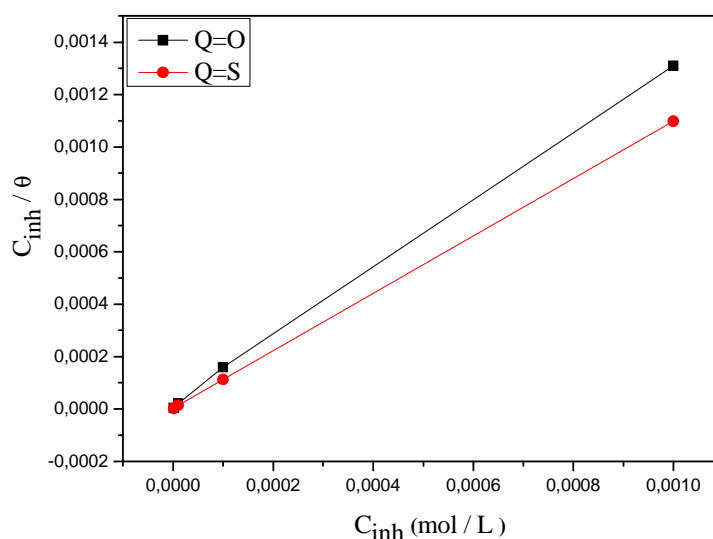


Figure 3. Langmuir adsorption of Q=S and Q=O on the steel surface in 0.5M H_2SO_4 solution

Table 2: Thermodynamic parameters for the adsorption of mild steel in 0.5M H_2SO_4 at 308K

Inhibitor	slope	$K_{ads}(\text{M}^{-1})$	R^2	$\Delta G_{ads}^\circ(\text{kJ mol}^{-1})$
Q=S	1.09593	475215.15	0.99998	-43.73
Q=O	1.2992	80762.39	0.99996	-39.20

3.3. Electrochemical impedance spectroscopy (EIS) studies:

Corrosion inhibition of mild steel in 0.5M H_2SO_4 solution with and without inhibitor was investigated by electrochemical impedance spectroscopy measurements. The nyquist representations of impedance behavior of mild steel in 0.5M H_2SO_4 with and without addition of different concentrations of quinoline are shown in the figures 4 and 5 It is observed from the fig. that at all concentration range of cloxacillin one large capacitive loop at higher frequency range followed by the one small inductive loop at lower frequency range.

The diameter of the circle increased with increase in inhibitors concentration. The higher frequency capacitive loop is due to the adsorption of inhibitors molecules [9]. Many workers also explained the results by using Randle circuit [10]. The deviation from the perfect semi-circle shape (depression) is often referred to the frequency dispersion of interfacial impedance. This behavior is due to the in homogeneity of the metal surface arising from surface roughness or interfacial phenomena [11]. It is observed that addition of inhibitor increases the values of R_{ct} and reduces the C_{dl} value. The decrease in C_{dl} is due to increase in thickness of the electronic double layer [12]. The increase in R_{ct} values is due to the formation of protective film on the metal/solution interface [13]. This observation suggests that quinoline molecules function by adsorption on metal surface and thereby causing the decrease in C_{dl} values and increase in R_{ct} values. The charge transfer resistance (R_{ct}) values and the interfacial double layer capacitance (C_{dl}) values calculated from the curves are shown in the **table 3**.

Table 3. Impedance parameters for corrosion of steel in 0.5 M H_2SO_4 in the absence and presence of different concentrations of Q=O and Q=S at 308 K

Inhibitor	Concentration (M)	R_t ($\Omega.cm^2$)	C_{dl} ($\mu f/cm^2$)	E (%)
0.5 M H_2SO_4	--	12	134	--
Q=S	10^{-6}	22	109	45
	10^{-5}	38	66	68
	10^{-4}	97	64	88
	10^{-3}	121	52	90
Q=O	10^{-6}	16.5	150	27
	10^{-5}	21	130	43
	10^{-4}	30	123	60
	10^{-3}	46	85	74

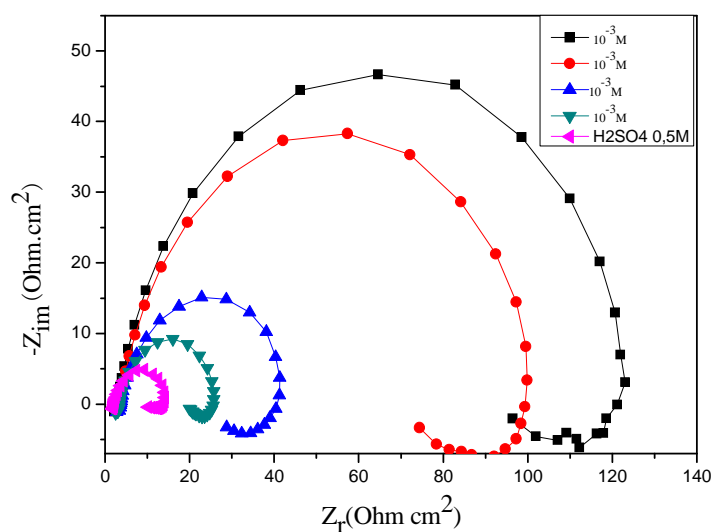


Figure 4 : Nyquist impedance diagram for mild steel in 0.5 M H_2SO_4 with inhibitor Q=S

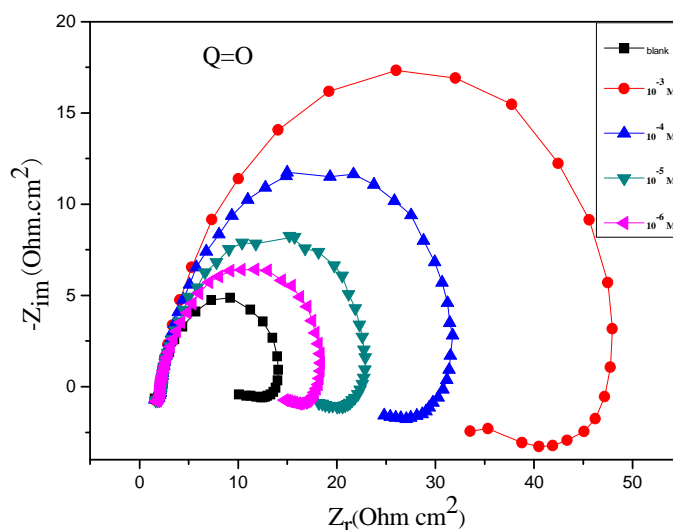


Figure 5: Nyquist impedance diagram for mild steel in 0.5 M H₂SO₄ with inhibitor Q=O

3.4. Tafel polarization study

Potentiodynamic polarization curves of mild steel in 0.5 M H₂SO₄ containing Q=S and Q=O at 308K are shown in Figure 6 and 7, respectively. In all cases, addition of each compound causes a remarkable decrease in the corrosion rate i.e., shifts the both anodic and cathodic curves to lower current densities. In other words, both cathodic and anodic reactions of mild steel electrode are drastically inhibited by the quinoline compounds. It should be noted that in anodic domain, it is difficult to recognize the linear Tafel regions. Accordingly, the corrosion current density values are estimated accurately by extrapolating the cathodic linear region back to the corrosion potential. Similar fitting method has also been widely used [14]. The electrochemical corrosion parameters including corrosion current densities (I_{corr}), corrosion potential (E_{corr}), cathodic Tafel slope (β_c) and corresponding inhibition efficiency (E_p) are given in Table 4.

Table 4. Polarization data of mild steel in 0.5 M H₂SO₄ without and with addition of inhibitors at 308 K

Inhibitors	Concentration (M)	-E _{corr} (mV/SCE)	I _{corr} (μ A/cm ²)	- β_c (mV/dec)	E _p (%)
0.5 M H ₂ SO ₄	--	-453	1647	-215	--
Q=S	10 ⁻⁶	-462	849	-184	48
	10 ⁻⁵	-465	523	-181	68
	10 ⁻⁴	-461	280	-173	87
	10 ⁻³	-461	162	-165	90
Q=O	10 ⁻⁶	-455	1168	-218	29
	10 ⁻⁵	-459	1025	-202	38
	10 ⁻⁴	-454	649	-194	61
	10 ⁻³	-451	392	-162	76

It is apparent that I_{corr} decreases considerably in the presence of each inhibitors, and decreases with increasing the inhibitors concentration. Correspondingly, E_p increases with the inhibitors concentration, due to the increase in the blocked fraction of the electrode surface by adsorption. E_p of 10⁻³ M inhibitor reaches up to a maximum of 90% for Q=S and 76% for Q=O, which again confirms that all two quinoline derivatives are good inhibitors in 0.5 M H₂SO₄, and E_p follows the order: Q=S > Q=O.

The presence of Q=S or Q=O does not prominently shift the corrosion potential, which indicates all studied quinoline derivatives act as cathodic-type inhibitors [15]. Furthermore, in the presence of each inhibitor, the slight change of β_c indicates that the cathodic corrosion mechanism of steel does not change.

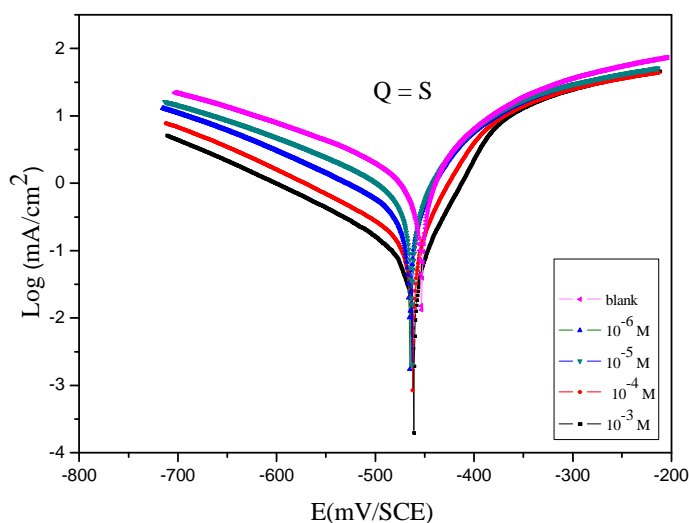


Figure 6 :polarization curves for mild steel in 0.5 M H₂SO₄ for various concentrations of Q=S at 308 K

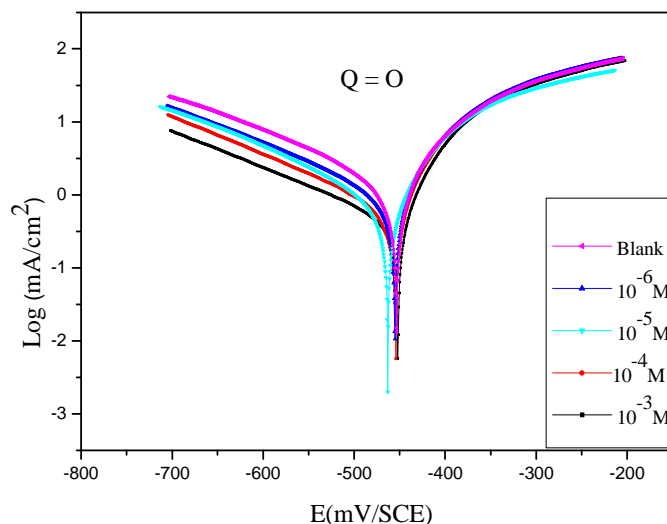


Figure 7. Polarization curves for mild steel in 0.5 M H₂SO₄ for various concentrations of Q=O at 308 K

3.5. Quantum chemical calculations

Frontier orbital theory is useful in predicting adsorption centers of the inhibitor molecules responsible of the interaction metallic surface/molecule [16-17]. The terms involving the frontier molecular orbitals (FMO) could provide dominative contribution, because of the inverse dependence of stabilization energy on orbital energy difference ($\Delta E = E_{LUMO} - E_{HOMO}$). The HOMO energy (E_{HOMO}) is often associated to the electron donating ability of the molecule, therefore, inhibitors with high values of E_{HOMO} have a tendency to donate electrons to appropriate acceptor with low empty molecular orbital energy. Conversely, the LUMO energy (E_{LUMO}) indicates the electron accepting ability of the molecule, the lowest its value the higher the capability of accepting electrons. The gap energy between the frontier orbitals (ΔE) is another important factor in describing the molecular activity, so when the gap energy decreased, the inhibitor efficiency is improved [19]. Elmsellem has investigated the adsorption of pyrimidin and their derivatives on mild steel surface in HCl acid medium and he has found that the gap energy decreases with increasing of inhibition efficiency [20].

The calculated quantum chemical parameters related to the inhibition efficiency of the studied molecules, such as the FMO energies (E_{HOMO} , E_{LUMO}), the gap energy (ΔE), the dipole moment (μ) are collected in Table 5.

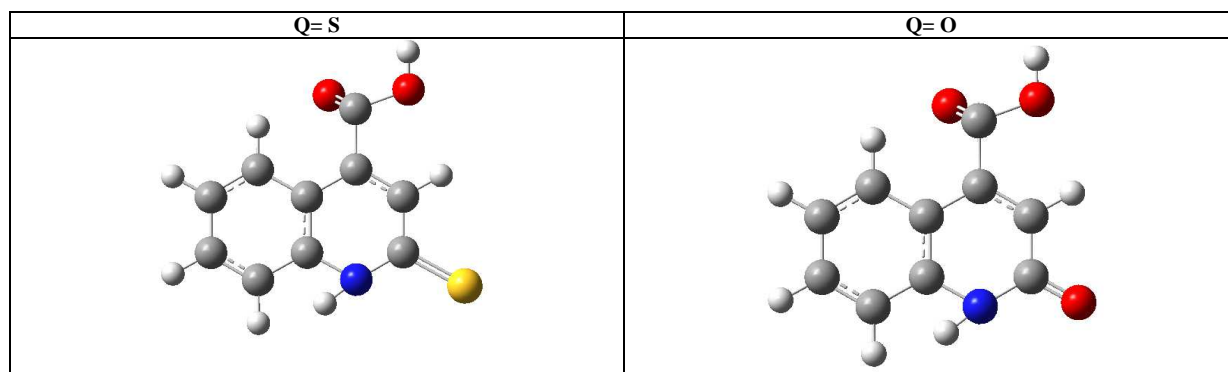


Figure 8. Quantum chemical descriptors of the studied inhibitors DFT at the B3LYP/6-31G(d, p)

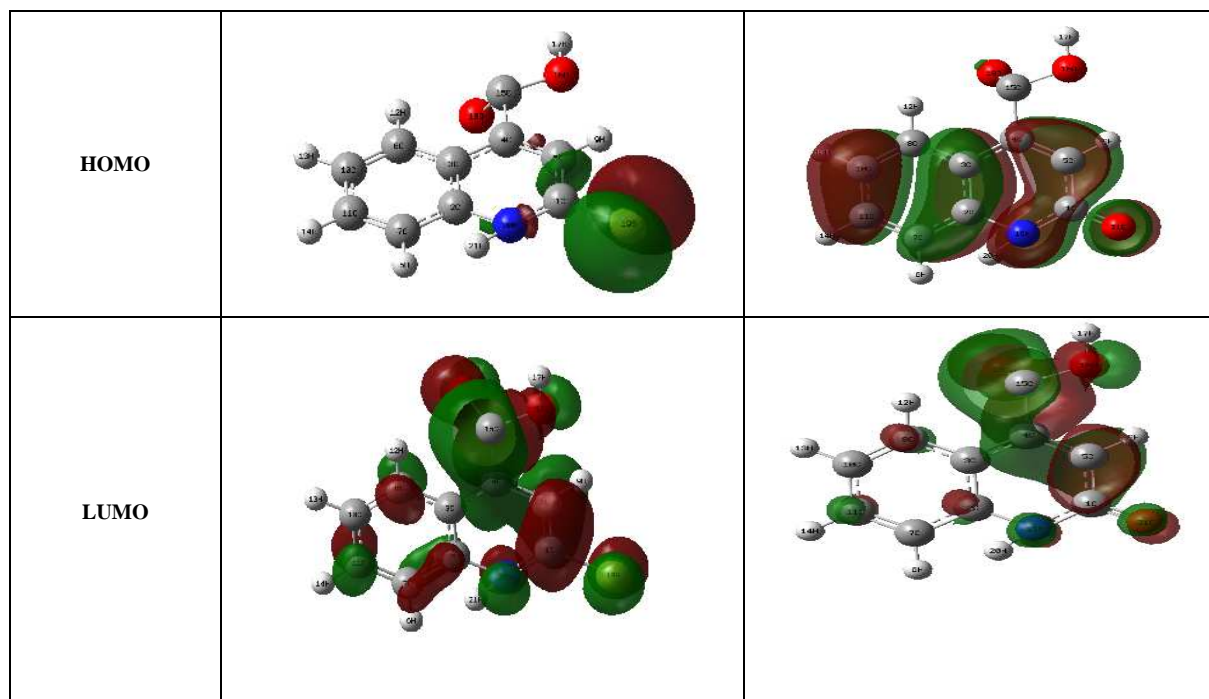


Figure 9. Optimized molecular structures HOMO and LUMO distribution for Q = S and Q = O

Table 5. The calculated quantum chemical parameters of Q = S and Q = O

Prameters	Q = S	Q = O
E_{HOMO} (eV)	-8.2710874	-9.24718184
E_{LUMO} (eV)	-2.1878448	-1.87327408
ΔE (eV)	6.0832426	7.37390776
μ (debye)	7.1421	4.6908

It is seen that the highest E_{HOMO} is obtained for Q = S, this result is not sufficient to conclude that Q = S is more efficient than P1. Therefore, the high values of E_{HOMO} are likely to indicate a tendency of the molecule to donate electrons to appropriate acceptor molecules with low empty molecular orbitals. Indeed, the excellent corrosion inhibitors are usually the organic compounds which not only give electrons to the unoccupied orbital of metal, but also to accept free electrons from it [21]. Thus, the E_{LUMO} and gap energy values obtained for Q = S show that it has the highest inhibition efficiency. This result is in good agreement with the experimental efficiency E (%) (Table 5). The dipole moment (μ) provides information on the polarity of the whole molecule. High dipole moment values are reported to facilitate adsorption (and therefore inhibition) by influencing the transport process through the adsorbed layer [22]. The dipole moments of Q = S and Q = O are 7.1421D and 4.6908D, respectively, which are higher than that of H₂O ($\mu = 1.88$ D). The high dipole moment value of these compounds probably indicates strong dipole-dipole interactions between them and metallic surface [23-24]. Accordingly, the quinoline molecules adsorption in aqueous solution can be regarded as a quasi-substitution process of the water molecules by the inhibitors molecules at metal surface (H₂O_{ads}).

CONCLUSION

The inhibition efficiency of mild steel corrosion in 1 M HCl by quinoline derivatives has been investigated using electrochemical measurement and quantum chemical calculations at (DFT/B3LYP/6-31 G (d, 2)) level of theory. The following conclusions were drawn from this study:

- (1) Two quinoline derivatives of $Q = S$ and $Q = O$ act as good inhibitors for the corrosion of mild steel in 0.5 M H₂SO₄ solution.
- (2) For each quinoline inhibitor, the adsorption is a spontaneous process and obeys Langmuir adsorption isotherm. The parameter of adsorption free energy (ΔG^0) indicates that the adsorption of inhibitor involves both chemisorption.
- (3) All quinoline compounds act as cathodic-type inhibitors in 0.5 M H₂SO₄. EIS spectra exhibit a large capacitive loop at high frequencies followed by a small inductive loop at low frequency values, and the presence of each inhibitor increases R_t values while reduces C_{dl} values.
- (4) The inhibition efficiency of two quinoline inhibitors follows the order: $Q = S > Q = O$.
- (5) Reasonably good agreement was observed between potentiodynamic polarization and electrochemical impedance spectroscopy techniques.
- (6) A good correlation was found between the quantum chemical parameters (ELUMO, gap energy (ΔE) and dipole moment (μ)) and inhibition efficiency.
- (7) The density distributions of the frontier molecular orbitals (HOMO and LUMO) show that $Q = S$ and $Q = O$ adsorb through the active centers nitrogen, oxygen, S and π electrons of the quinoline ring.

REFERENCES

- [1] I. El Mounsi, H. Elmsellem, A. Aouniti, H. Bendaha, M. Mimouni, T. Benhadda, R. Mouhoub, B. El Mahi, A. Salhi and B. Hammouti. *Der Pharma Chemica*, **2015**, 7(10), 350-356.
- [2] F.Aouinti, H.Elmsellem, A.Bachiri, M.L.Fauconnier, A.Chetouani, b.Chaouki, A.Aouniti, B.Hammouti, *Journal of Chemical and Pharmaceutical Research*, **2014**, 6(7),10-23.
- [3] M. Ramdani, H. Elmsellem, N. Elkhiati, B. Haloui, A. Aouniti, M. Ramdani, Z. Ghazi, A. Chetouani and B.Hammouti. *Der Pharma Chemica*, **2015**, 7(2), 67-76.
- [4] M.J.Frisch,G.W.Trucks,H.B.Schlegel et al., Gaussian 09, Revision A.1, Gaussian, Inc., Wallingford, Conn, USA, **2009**.
- [5] H. Elmsellem, H. Nacer, F. Halaimia, A. Aouniti, I. Lakehal, A. Chetouani, S. S. Al-Deyab, I. Warad, R. Touzani, B. Hammouti, *Int. J. Electrochem. Sci*, **2014**, 9, 5328-5351.
- [6] N.Saidi, H.Elmsellem, M.Ramdani, A.Chetouani, K.Azzaoui, F.Yousfi, A.Aounitia and B. Hammouti, *Der Pharma Chemica*, **2015**, 7(5):87-94.
- [7] N.K.Sebbar, H.Elmsellem, M.Boudalia, S.lahmidi, A.Belleaouchou, A.Guenbour, E. M.Essassi, H.Steli, A.Aouniti, *J. Mater. Environ. Sci*, **2015**, 6 (11), 3034-3044.
- [8] Y. El Ouadi, H. Elmsellem, M. El fal, N. K. Sebbar, A. Bouyanzer, R. Rmili, E. M. Essassi, B. El Mahi, L. Majidi & B. Hammouti, *Der Pharma Chemica*, **2016**, 8(1),365-373.
- [9] H. Elmsellem, H. Nacer, F. Halaimia, A. Aouniti, I. Lakehal, A. Chetouani, S. S. Al-Deyab, I. Warad, R. Touzani, B. Hammouti. *Int. J. Electrochem. Sci*, **2014**, 9, 5328.
- [10] N. K. Sebbar, H. Elmsellem, M. Ellouz, S. Lahmidi, E. M. Essassi, I. Fichtali, M. Ramdani, A. Aouniti, A. Brahimi and B. Hammouti. *Der Pharma Chemica*, **2015**, 7(9):33-42.
- [11] H. Elmsellem, H. Bendaha, A. Aouniti, A. Chetouani, M. Mimouni, A. Bouyanzer, *Mor. J. Chem*, **2014**, 2 (1), 1-9.
- [12] H.Elmsellem, T.Harit, A.Aouniti, F.Malek, A.Riahi, A.Chetouani, B.Hammouti, *Protection of Metals and Physical. Chemistry of Surfaces*, **2015**, 51(5), 873.
- [13] H.Elmsellem, A.Elyoussfi, H.Steli, N. K.Sebbar, E. M.Essassi, M.Dahmani, Y.El Ouadi, A.Aouniti, B.El Mahi, B.Hammouti, *Der Pharma Chemica*, **2016**, 8(1), 248-256.
- [14] H. Elmsellem, K. Karrouchi, A. Aouniti, B. Hammouti, S. Radi, J. Taoufik, M. Ansar, M. Dahmani, H. Steli and B. El Mahi, *Der Pharma Chemica*, **2015**, 7(10), 237-245.
- [15] A. L.Essaghouani, H.Elmsellem, M.Ellouz, M.El Hafi, M.Boulhaoua, N. K.Sebbar, E. M.Essassi, M.Bouabdellaoui, A.Aouniti and B.Hammouti, *Der Pharma Chemica*, **2016**, 8(2) 297-305.
- [16] I.Chakib, H.Elmsellem, N. K.Sebbar, E. M.Essassi, I.Fichtali, A.Zerzouf, Y.Ouzidan, A.Aouniti, B. El Mahi and B.Hammouti, *Der Pharma Chemica*, **2016**, 8(2) 380-391.
- [17] H. Elmsellem, A. Aouniti, M.H. Youssoufi, H. Bendaha, T. Ben hadda, A. Chetouani, I. Warad, B. Hammouti, *Phys. Chem. News*, **2013**, 70, 84.
- [18] A. Aouniti, H. Elmsellem, S. Tighadouini, M. Elazzouzi, S. Radi, A. Chetouani, B. Hammouti, A. Zarrouk, *Journal of Taibah University for Science*, **2015**, <http://dx.doi.org/10.1016/j.jtusci.2015.11.008>.

-
- [19] H. Elmsellem, M. H. Youssouf, A. Aouniti, T. Ben Hadd, A. Chetouani, B. Hammouti. *Russian, Journal of Applied Chemistry*, **2014**, 87(6), 744-753
- [20] H. Elmsellem, A. Aouniti, M. Khoutou, A. Chetouani, B. Hammouti, N. Benchat, R. Touzani and M. Elazzouzi, *J. Chem. Pharm. Res.*, **2014**, 6, 1216.
- [21] A. L. Essaghrouani, H. Elmsellem, M. Boulhaoua, M. Ellouz, M. El Hafi, N. K. Sebbar, E. M. Essassi, M. Bouabdellaoui, A. Aouniti and B. Hammouti., *Der Pharma Chemica*, **2016**, 8(2):347-355
- [22] I. Chakib, H. Elmsellem, N. K. Sebbar, E. M. Essassi, I. Fichtali, A. Zerzouf, Y. Ouzidan, A. Aouniti, B. El Mahi and B. Hammouti., *Der Pharma Chemica*, **2016**, 8(2):422-433.
- [23] N. K. Sebbar, H. Elmsellem, M. Ellouz, S. Lahmidi, A. L. Essaghrouani, E. M. Essassi, M. Ramdani, A. Aouniti, B. El Mahi and B. Hammouti. *Der Pharma Chemica*, **2015**, 7(10), 579-587.
- [24] H. Elmsellem, N. Basbas, A. Chetouani, A. Aouniti, S. Radi, M. Messali, B. Hammouti, *Portugaliae. Electrochimica. Acta.*, **2014**, 2, 77.